Electronic structure of lithium amide

N. Kamakura,[1] Y. Takeda,[1] Y. Saitoh,[1] H. Yamagami,[1,2] M. Tsubota,[3,*] B. Paik,[3] T. Ichikawa,[3] Y. Kojima,[3]
T. Muro,[4] Y. Kato,[4] and T. Kinoshita[4]

[1]*Condensed Matter Science Division, Japan Atomic Energy Agency, Hyogo 679-5148, Japan*
[2]*Department of Physics, Kyoto Sangyo University, Kyoto 603-8555, Japan*
[3]*Institute for Advanced Materials Research, Hiroshima University, Higashi-Hiroshima 739-8530, Japan*
[4]*Japan Synchrotron Radiation Research Institute, SPring-8, Hyogo 679-5198, Japan*

The electronic structure of the insulator lithium amide ($LiNH_2$), which is a lightweight complex hydride being considered as a high-capacity hydrogen storage material, is investigated by N $1s$ soft x-ray emission spectroscopy (XES) and absorption spectroscopy (XAS). The XES and XAS spectra show a band gap between the valence and conduction bands. The valence band in the XES spectrum consists of three peaks, which extend up to ~ -8 eV from the valence band top. The band calculation within the local-density approximation (LDA) for $LiNH_2$ shows energetically separated three peaks in the occupied N $2p$ partial density of states (pDOS) and the band gap. The energy distribution of three peaks in the XES spectrum agrees with that in the calculated pDOS except for the peak at the highest binding energy, which is attributed to the strongly hybridized state between N $2p$ and H $1s$. The XES experiment has clarified that the strongly hybridized state with H $1s$ in $LiNH_2$ is located at binding energy higher than that of the LDA calculation, while the overall feature of the electronic structure of $LiNH_2$ experimentally obtained by XES and XAS is consistent with the calculated result.

PACS number(s): 71.20.Ps, 78.70.En, 78.70.Dm

Recently lightweight hydrides have been extensively investigated as candidates for high-performance hydrogen storage materials.[1–7] In the lightweight hydrides, an indispensable issue for the practical application as hydrogen storage materials is to control the absorption and desorption of hydrogen under moderate conditions of temperature and pressure. The stability of the hydrides is described by the formation enthalpy, which results from the electronic structure. The enthalpy change controls the equilibrium H_2 pressure and temperature via the van't Hoff relation.[8]

Lithium amide is one of the lightweight complex hydrides receiving much attention recently as a promising high-capacity hydrogen storage material.[1–5] In $LiNH_2$, the two H atoms covalently bond with the N atom, which forms the amide ion $[NH_2]^-$, and the amide ion $[NH_2]^-$ ionically bonds with Li. Thus, the formation enthalpy of $LiNH_2$ is low compared to that of the hydrides of hydrogen storage intermetallic compounds formed by the metallic bond.[8] Owing to its stability, the hydrogenation and dehydrogenation in $LiNH_2$ proceed through chemical reactions and the formation of a new compound with stoichiometric compositions, in contrast to the hydrogen absorption and desorption in hydrogen storage inter-metallic compounds, where hydrogen occupies the interstitial sites also with nonstoichiometric compositions and the original structure of the host metal is almost unchanged in most cases. In the Li-based lightweight hydrides, the following two-step reversible reaction among Li_3N, Li imide (Li_2NH), Li amide ($LiNH_2$), and Li hydride (LiH) has been reported to be able to absorb and desorb hydrogen with the high mass content 10.4 wt%:[1–5]

$$Li_3N + 2H_2 \leftrightarrow Li_2NH + LiH + H_2 \leftrightarrow LiNH_2 + 2LiH.$$

The second reaction is considered to proceed via two elementary reaction steps, where decomposition of $LiNH_2$ to Li_2NH and NH_3 in the first step is followed by the second step of LiH with NH_3 to form H_2 and $LiNH_2$.[2–5] It is important to note that in the preceding chemical reaction, the hydrogen desorption of lithium amide occurs at a relatively high temperature compared to that of hydrogen storage intermetallic compounds, because of the low reaction enthalpy among the Li-based lightweight hydrides. The further improvement of the hydrogen absorption and desorption property may be proposed from the knowledge of the electronic structure, which predominantly contributes to the formation enthalpy. Thus, the accurate description of the electronic structure based on the experimental and theoretical studies is useful for the control and improvement of hydrogenation-dehydrogenation properties.

Among the hydrides, the detailed experimental study of the electronic structure has been performed only on metal hydrides, so far, and these studies have clarified characteristics of the electronic structure of the metal hydrides.[8–13] In the rare-earth and transition metal hydrides, the hydrogen-induced state by the hybridization between the metal-derived states and the H $1s$ states is formed at the high binding energy side of the metal d band.[8–13] The hydrogen-induced state has been experimentally observed from about -4 to -8 eV binding energies by photoemission spectroscopy.[8,9,11–13] Although the electronic states of the metal hydrides as represented by the hydrogen-induced state show the band dispersion, the complex hydride $LiNH_2$ is considered to be an ionic insulator. Thus, the electronic structure of $LiNH_2$ is of particular interest also from the fundamental point of view in terms of the bonding state of hydrogen in lightweight complex hydrides that is different from the metal hydride system. However, the experimental knowledge of the electronic structure of the lightweight hydride is fairly limited, since the insulating nature of the lightweight complex hydride prevents the investigation of the electronic structure by photoemission spectroscopy. Thus, the electronic structure of $LiNH_2$ has not been clarified experimentally. In this work, we have studied, for the first
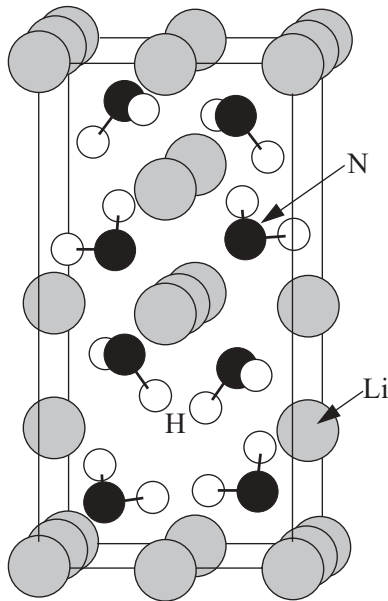
FIG. 1. Crystal structure of $LiNH_2$. The large circle indicates Li atom. The small solid and open circles are N and H atoms, respectively.

FIG. 2. (Color online) (a) N $1s$ XES and XAS spectra for $LiNH_2$. The peaks in the XES spectrum are marked with A, B, and C. Those in the XAS spectrum are labeled with D, E, and F. The top axis shows the energy relative to the valence band top. (b) Calculated N $2p$ pDOS (upper panel) and total DOS (lower panel) with the broadening curves of the calculated DOSs by the convolution of the Gaussian and Lorentzian are indicated for the comparison with the experimental result.

time, the electronic structure of $LiNH_2$ by N $1s$ soft x-ray emission spectroscopy (XES) and N $1s$ soft x-ray absorption spectroscopy (XAS) in fluorescence yield mode, enabling us to probe the electronic structure even for the insulator due to the photon in-photon out probe. The N $2p$ partial density of states (pDOS) of $LiNH_2$ can be experimentally obtained by the XES and XAS measurements using the N $1s$ core level. The experimentally obtained spectra for $LiNH_2$ have been compared to the N $2p$ pDOS calculated in the local-density approximation (LDA).[14] From comparison between the experimental spectra and the calculation, the electronic structure of $LiNH_2$ has been investigated.

The experiments were performed at soft x-ray beam line BL27SU of SPring-8. The N $1s$ XES experiment of $LiNH_2$ was performed with a grazing incidence flat-field spectrometer.[15] The N $1s$ XAS spectrum was measured using fluorescence yield. These XES and XAS measurements were done for a lithium amide sample of a few mm^3 size at room temperature. The crystal symmetry of lithium amide is tetragonal space group $I\bar{4}$ (Fig. 1) with lattice parameters $a = b = 5.034$ Å and $c = 10.256$ Å. The frame of lithium amide crystal is formed by Li, which is considered to provide the electron charge to the amide ion $[NH_2]^-$. In the amide ion $[NH_2]^-$ of $LiNH_2$, the N–H bonding length is 0.986 Å and 0.942 Å, and the N–H–N bonding angle is 99.97°.[16] The first-principles calculation has been performed using the all-electron full-potential-linear-augmented-plane-wave (FLAPW) method to compare the DOS obtained by the XES and XAS experiments. The Kohn–Sham equations are iteratively solved in a scalar-relativistic approximation with the FLAPW method. For the self-consistent calculation the **k**-sample points are generated by $4 \times 4 \times 4$ uniform mesh in the Brillouin zone. The muffin-tin radii are set to be 0.79, 0.53, and 0.41 Å for the Li, N, and H atoms, respectively.

Figure 2(a) shows the N $1s$ XES and XAS spectra for $LiNH_2$. The XES spectrum exhibits a three-peak structure which extends up to about -8 eV from the top of valence band. These three peaks labeled A, B, and C are quite sharp, which is the feature of the occupied electronic states of $LiNH_2$. The peak at the bottom of the conduction band in the XAS spectrum (peak D) is separated from the peak of the valence band top (peak C) by the band gap of $LiNH_2$. The structure above the valence band top in the XES spectrum is possibly attributed to impurities in the probing region. For detailed discussion, the theoretical total DOS and pDOS for each atom of $LiNH_2$ are shown in Fig. 3, which is consistent with reported calculations.[16,17] The features of the calculated DOS of $LiNH_2$ in Fig. 3 are as follows: The band gap between the occupied valence band and the unoccupied conduction band is predicted to be 3.33 eV. The occupied part of the calculated total DOS of $LiNH_2$ shows four features (peaks). The energetically separated sharp DOS features of the occupied valence band are also theoretically predicted to be the characteristics of the electronic states of the ionic insulator $LiNH_2$ distinct from those of metal hydrides. Among the four features, the peak at ~-15 eV originates from the hybridization between the N $2s$ and H $1s$ states. This feature is surely negligible in the XES spectrum. It is found from Fig. 3 that the other three peaks up to ~-6.5 eV in the theoretical total DOS are similar to those of the N $2p$ pDOS. These three DOS peaks, which correspond to peaks A, B, and C in the XES spectrum, are located at -5.0 to -6.43 eV, -1.95 to -3.19 eV, and 0 to -1.24 eV,
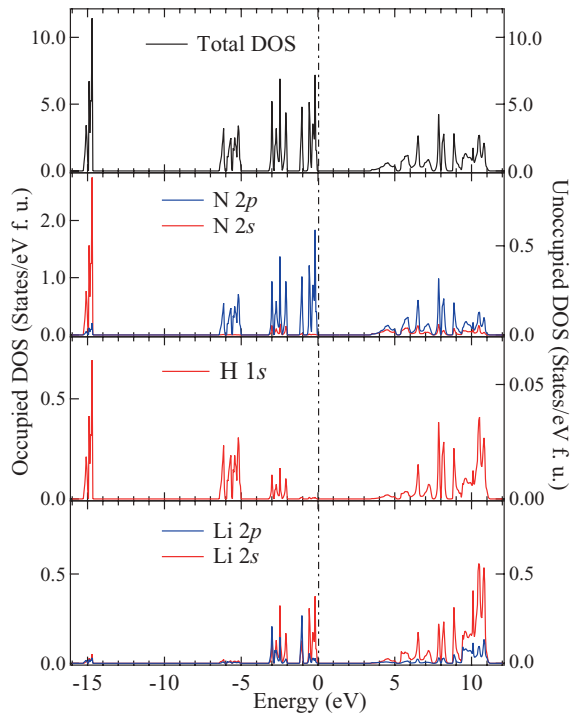
FIG. 3. (Color online) Calculated total DOS and pDOSs for Li, N, and H of LiNH$_2$.

respectively, in the calculation (Fig. 3). As shown in Fig. 3, the states corresponding to peak A in the XES spectrum originate from the strong hybridization between the N 2p and H 1s states by the covalent bond between N and H in LiNH$_2$. In the middle energy peak corresponding to peak B, the N 2p state hybridizes with both the H 1s state and the Li-derived states. Peak C is predominantly formed by the N 2p states and is also slightly contributed to by the Li-derived states. The unoccupied part in the low energy region near the bottom of the conduction band is mainly contributed by the N- and Li-derived states as found from the N and Li pDOS in Fig. 3. The number of electrons for the Li atom is estimated to be 0.1028, which indicates that the Li atom donates the electron charge to the amide ion [NH$_2$]$^-$ and the ionic bond between Li and the amide ion [NH$_2$]$^-$. Figure 3 shows that the calculation predicts the dominant contribution of N 2p to the occupied and unoccupied states and the shape of the total DOS is almost identical to that of the N 2p pDOS except for the feature at ∼−15 eV. Thus, the dominant feature of the electronic states of LiNH$_2$ is expected to be investigated with N 1s XES and XAS spectra.

In Fig. 2(b), the calculations for the N 2p pDOS and total DOS are compared to the XES and XAS spectra. Here, the energy of the valence band top in the calculation is set to the origin. The occupied parts of these DOS are broadened for comparison with the XES spectrum by a convolution with a Lorentzian [full width at half maximum (FWHM) = 0.3 eV] for lifetime broadening followed by a Gaussian (FWHM = 0.43 eV) for the experimental resolution which is estimated by the width of the elastic peak.[18] The Gaussian width of the unoccupied part is set at FWHM = 0.13 eV of the resolution of the XAS. For the set of the energy level of the

experimental spectra, peak C in the XES spectrum is aligned with the peak at the valence band top after broadening of the calculated DOS (Fig. 2). Although the calculated DOS features of the occupied valence band of LiNH$_2$ are separated, these features are connected by the broadening of the calculated DOS, as observed in the XES spectrum. Figure 2 shows that the experimental N 2p pDOS measured by the N 1s XES and XAS is almost consistent with the theoretical curve simulated by broadening of the calculated DOS in terms of the three-peak structure in the occupied valence band and the existence of the band gap. Peaks A, B, and C in the XES spectrum are estimated to be located at −6.64, −2.19, and −0.18 eV relative to the origin, respectively. The relative energy between peaks B and C in the XES spectrum is consistent with the calculated result. As found from Fig. 2 and the estimated energies, however, the energy position of peak A in the XES spectrum deviates from the calculation. The calculated results show that peak A originates from the N 2p state strongly hybridized with the H 1s state. In the broadened curve of the calculated N 2p DOS, A is peaked at 5.42 eV. Thus, peak A in the XES spectrum is located at a binding energy 1.22 eV higher than that in the theoretical curve. The calculation of Fig. 3 shows that the occupied valence band predominantly consists of the electrons distributing on the amide ion [NH$_2$]$^-$ and is localized as found from the sharp DOS shapes. In fact, as predicted in the total DOS of LiNH$_2$ of Fig. 3, the molecular orbitals of the amide ion [NH$_2$]$^-$ occupied by the eight electrons already show that the energy splitting of the occupied states to the four levels is caused by the hybridization between the H 1s and N-derived states in the amide ion [NH$_2$]$^-$.[17] Thus, the DOS peaks in the occupied valence band are intense in Fig. 3. The XES experiment also shows the large contribution of peak A in the XES spectrum. Thus, the energy deviation of the N 2p state hybridized with the H 1s state from the calculation is noticeable. The N 1s XAS spectrum shows the spectral structure due to the unoccupied part of the N 2p pDOS. The peaks in the XAS spectrum are marked by D, E, and F in Fig. 2. In Fig. 2, the position of peak D located at the lowest energy in the unoccupied part deviates from the calculation. Peak D observed at 5.15 eV in the XAS spectrum is predicted to be 4.52 eV in the calculation, which reflects a wider band gap in the experiment.

In summary, we have studied the electronic structure of the lightweight complex hydride LiNH$_2$ by N 1s XES and XAS experiments. The XES and XAS spectra show the three-peak structure extending up to −8 eV in the occupied valence band and band gap between the valence and conduction bands. These features are almost consistent with the LDA calculation. Thus, the overall consistency in the electronic structure of LiNH$_2$ between the experimental result and the LDA calculation is confirmed. However, the detailed comparison indicates a deviation from the calculation in the strongly hybridized state between N 2p and H 1s. The XES spectrum shows that the hybridized state is located at a binding energy ∼1.2 eV higher than that of the calculated DOS. For the full understanding of the electronic structure of LiNH$_2$ in terms of the feature of the strongly hybridized states with the H 1s state, systematic studies on the electronic states of other amide hydrides are desirable.

---

[*]Present address: Institute of Materials Structure Science, High Energy Accelerator Research Organization (KEK), Tokai 319-1106, Japan.

[1]P. Chen, Z. Xiong, J. Luo, J. Lin, and K. L. Tan, Nature (London) **420**, 302 (2002).

[2]T. Ichikawa, S. Isobe, N. Hanada, and H. Fujii, J. Alloys Compd. **365**, 271 (2004).

[3]Y. Kojima and Y. Kawai, J. Alloys Compd. **395**, 236 (2005).

[4]S. Hino, N. Ogita, M. Udagawa, T. Ichikawa, and Y. Kojima, J. Appl. Phys. **105**, 023527 (2009).

[5]I. P. Jain, P. Jain, and A. Jain, J. Alloys Comp. **503**, 303 (2010).

[6]M. J. van Setten, V. A. Popa, G. A. de Wijs, and G. Brocks, Phys. Rev. B **75**, 035204 (2007).

[7]H. Saitoh, A. Machida, Y. Katayama, and K. Aoki, Appl. Phys. Lett. **93**, 151918 (2008).

[8]Y. Fukai, *The Metal-Hydrogen System: Basic Bulk Properties* (Springer-Verlag, Berlin, 2005).

[9]M. Gupta and L. Schlapbach, in *Hydrogen in Intermetallic Compounds I*, edited by L. Schlapbach (Springer, Berlin, 1988).

[10]M. Gupta and J. P. Burger, Phys. Rev. B **22**, 6074 (1980).

[11]D. J. Peterman, J. H. Weaver, and D. T. Peterson, Phys. Rev. B **23**, 3903 (1981).

[12]J. Hayoz, C. Koitzsch, M. Bovet, D. Naumović, L. Schlapbach, and P. Aebi, Phys. Rev. Lett. **90**, 196804 (2003).

[13]C. Koitzsch, J. Hayoz, M. Bovet, F. Clerc, L. Despont, C. Ambrosch-Draxl, and P. Aebi, Phys. Rev. B **70**, 165114 (2004).

[14]J. P. Perdew and Y. Wang, Phys. Rev. B **45**, 13244 (1992).

[15]T. Tokushima, Y. Harada, M. Watanabe, Y. Takata, E. Ishiguro, A. Hiraya, and S. Shin, Surf. Rev. Lett. **9**, 503 (2002).

[16]J. B. Yang, X. D. Zhou, Q. Cai, W. J. James, and W. B. Yelon, Appl. Phys. Lett. **88**, 041914 (2006).

[17]T. Tsumuraya, T. Shishidou, and T. Oguchi, J. Phys. Condens. Matter **21**, 185501 (2009).

[18]C. B. Stagarescu, L.-C. Duda, K. E. Smith, J. H. Guo, J. Nordgren, R. Singh, and T. D. Moustakas, Phys. Rev. B **54**, 17335(R) (1996).